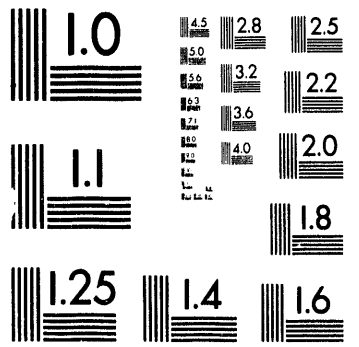
1.0
1.1
1.25
1.4
1.6
1.8
2.0
2.2
2.5
2.8
3.2
3.6
4.0
4.5
5.0
5.6
6.3
7.1
8.0

1 of 1

Category Distribution
UC-261

SAND93-1900
Unlimited Release
Printed October 1993

User's Guide for the Frequency Domain Algorithms in the LIFE2 Fatigue Analysis Code

H. J. Sutherland

Wind Energy Technology Department
Sandia National Laboratories
Albuquerque, NM 87185

and

R. L. Linker

New Mexico Engineering Research Institute
Albuquerque, NM 87106

ABSTRACT

The LIFE2 computer code is a fatigue/fracture analysis code that is specialized to the analysis of wind turbine components. The numerical formulation of the code uses a series of cycle count matrices to describe the cyclic stress states imposed upon the turbine. However, many structural analysis techniques yield frequency-domain stress spectra and a large body of experimental loads (stress) data is reported in the frequency domain. To permit the analysis of this class of data, a Fourier analysis is used to transform a frequency-domain spectrum to an equivalent time series suitable for rainflow counting by other modules in the code. This paper describes the algorithms incorporated into the code and their numerical implementation. Example problems are used to illustrate typical inputs and outputs.

TABLE OF CONTENTS

LIST OF FIGURES

INTRODUCTION

The analysis of the fatigue lifetime of a component of a Wind Energy Conversion System (WECS) requires that the stress state imposed upon that component be formulated in terms of stress cycles. However, many structural analysis techniques yield frequency-domain stress spectra and a large body of experimental loads (stress) data is reported in the frequency domain. To permit the analysis of this class of data, a set of Fourier analysis modules have been added to the LIFE2 fatigue/fracture analysis code [1]. The computational framework for these modules follows the work of Akins [2]. Simply stated, the modules convert frequency-domain stress data into time-series data (stress-time history) suitable for analysis by a cycle counting algorithm that converts the time-series data into stress cycles. A typical algorithm, commonly called the rainflow algorithm, has been incorporated in LIFE2 code previously by Schluter and Sutherland [3].

As reported by Sutherland [4,5] and Sutherland and Osgood [6], the analysis of the frequency spectrum by the LIFE2 code may take one of two forms. In the first technique, the entire frequency-domain stress spectra is used with a Fast Fourier Transforms (FFTs) and a random phase generator to synthesize a time series suitable for rainflow counting. In the second technique, the synthesis of time series data is based on the addition of deterministic (azimuth average) stresses to time-series data synthesized from frequency spectra data for the non-deterministic ("random") stresses. Both techniques may be applied to one and two dimensional stress states.

In this paper, we will present a discussion of the algorithms used in these analyses and their numerical implementation in the code. A set of examples are then used to describe the inputs and outputs for this analysis. Example input files are contained in the Appendices of this report.

FORMULATION

The algorithms incorporated into the LIFE2 code basically use an inverse Fourier transform to synthesize time series data that is suitable for rainflow counting. This section describes the numerical algorithms employed by the code to perform this synthesis. The first section describes the basic synthesis module, and the second section describes the synthesis of bi-axial time series data.

THE FFT ALGORITHM

To convert a frequency spectrum into a time series requires the use of an inverse Fourier transform. Several FFTs and their inverses have been written, e.g. see Reference 7, that specialize the Fourier transform and its inverse into a "fast" digital analysis. One such transform [8], with its accompanying pre- and post-processors, has been incorporated into the LIFE2 code.

The LIFE2 module assumes that the input frequency spectrum (i.e., the spectrum that is to be converted to an equivalent time series) is a uniform series of N components with a frequency interval of Δf. The spectrum is input as a series of positive amplitudes A_i and phase angles ϕ_i , i = 1, N. If a ϕ_i is not included in the input, a random number generator [9] is used to generate a random phase angle between 0 and 2π radians (see References 4, 5 and 6 for explanations and analyses of the use of random phase angles to synthesize "realistic" time series data for wind turbines). The FFT pre-processor reads the spectrum, generates random phases when required, and converts each phase into its sine and cosine components [$(A_i)_S$ and $(A_i)_C$, respectively] using the relations:

$$(A_i)_S = (A_i)\sin(\phi_i) \quad , \tag{1.1}$$

and,

$$(A_i)_C = (A_i)\cos(\phi_i) \quad . \tag{1.2}$$

The i^{th} component of the spectrum corresponds to a frequency of:

$$f_i = (i-1)\,\Delta f \quad , \text{where } i = 1, \ldots, N \tag{1.3}$$

To speed processing, the mean stress (the zero frequency component A_1) is set equal to zero and the number of components in the spectrum, N, is set to an integer power of 2; i.e.,

$$A_1 = (A_1)_S = (A_1)_C = 0 \quad , \tag{1.4}$$

and

$$N = 2^m \quad , \text{where m is a positive integer.} \tag{1.5}$$

If the input value of N is not a power of 2, the additional components in the amplitude spectrum are set equal to zero.

The inverse FFT algorithm converts this frequency spectrum into a time series [7]. The output time series is a uniform series, with the time increment, $\Delta\tau$, given by:

$$\Delta\tau = \frac{1}{2\,N\,(\Delta f)} \quad . \tag{1.6}$$

The FFT post-processor adds the mean stress to the time series and writes the results to file in a format suitable for analysis by the rainflow counter in the LIFE2 code [3]. The output time series has a total time length T equal to

$$T = 2N\Delta\tau = \frac{1}{\Delta f} \quad . \tag{1.7}$$

Variation of the RMS

Typically, frequency spectra from wind turbines are not constant in time; rather, the frequency spectra vary about some average frequency spectrum because of turbulence in the inflow to the turbine. To permit the LIFE2 code to synthesize time series data from the average spectrum, an algorithm was incorporated into the code that systematically varies the mean root-mean-square, RMS, of the average frequency spectrum, $(RMS)_m$, over a defined range in even increments.

The algorithm varies the mean RMS of the input frequency spectrum by multiplying all amplitudes in the mean frequency spectrum, $(A_i)_m$, by the factors $(r_a)_j$; namely:

$$A_i = (r_a)_j (A_i)_m \quad , \text{where } i = 1, \ldots, N \text{ and } j = 1, \ldots, J. \tag{1.8}$$

For the frequency synthesis procedure used in the LIFE2 code, $(r_a)_j$ is defined by a single input variable R_a. For J steps,* $(r_a)_j$ is given by

$$(r_a)_j = (R_a)_{min} + (j-1)\Delta R_a \quad , \text{where } j = 1, \ldots, J \text{ and } J > 1 \quad . \tag{1.9}$$

The variables in this equation are defined in terms of the input variable R_a to be

$$(R_a)_{min} = \begin{cases} 0.05 & \text{for } R_a \geq 0.95 \\ 1 - R_a & \text{for } R_a < 0.95 \end{cases} \quad , \tag{1.10}$$

$$\Delta R_a = \frac{(R_a)_{max} - (R_a)_{min}}{J-1} \quad , \tag{1.12}$$

and

* The numerical value for J is not intuitatively obvious. As described in References 4, 5 and 6, values between 1 and 100 have been used for the value of J for typical problems. Based on this previous experience, a value of 10 typically permits the LIFE2 code to accurately simulate cycle counts using the average frequency spectrum.

$$(R_a)_{max} = 1 + R_a \quad . \tag{1.11}$$

For the special case of J =1,

$$(r_a)_j = (r_a)_1 = (R_a)_{max} \quad . \tag{1.13}$$

This formulation implies that the RMS for the adjusted amplitude spectrum at interval j, $[(RMS)_a]_j$, becomes:

$$\left[(RMS)_a\right]_j = \sqrt{\sum_{i=1}^{N} \frac{\left[(r_a)_j\,(A_i)_m\right]^2}{2}} \quad , \tag{1.14}$$

$$\left[(RMS)_a\right]_j = (r_a)_j \sqrt{\sum_{i=1}^{N} \frac{\left[(A_i)_m\right]^2}{2}} \quad , \tag{1.15}$$

$$\left[(RMS)_a\right]_j = (r_a)_j\,(RMS)_m \quad . \tag{1.16}$$

Thus, the RMS of the amplitude spectrum is also changed by a factor of $(r_a)_j$.

As described by Equations (1.9) through (1.13), $(r_a)_j$ is varied symmetrically about 1.0 for values of R_a less than 0.95 and J > 1. The lower bound of 0.05 on $(R_a)_{min}$ was chosen because very low values of $(r_a)_j$ produce very small stresses, which are not consistent with physical reality.

Spectral Analysis with Random Phase Angles

Typically, frequency spectra from wind turbines contain two classes of components. The first is the deterministic (azimuth average or harmonic) component and the second is the non-deterministic (random) component. The deterministic component is obtained by averaging the time series data as a function of rotor position (the azimuth-average). The second component of the total spectrum is a random variation about the azimuth-average, deterministic component. The random components of the frequency spectrum imply that the synthesis of a time series from a frequency spectrum for wind turbines is not a unique process.

Akins [2] handled the synthesis of both signals using the average amplitude spectrum with a random phase angle for each amplitude. He suggests that a synthesized time series would be closer to an actual measured time series if the phase angles for the azimuth-average components of the spectra are included in the synthesis; i.e., because the phase angles for azimuth-average components are essentially constant, they should be included in the synthesis process. He further suggests that the random components are best described using the average amplitude spectrum with random phases.

The concept of fixed and random phase angles has been incorporated into the LIFE2 algorithms using variable input parameters. In the first class of inputs, the amplitude spectrum input into the algorithm is assumed to contain both deterministic and non-deterministic components. We will refer to this analysis as a "Total Spectral Analysis." For the second, the two components are divided from one another. We will refer to this analysis as a "Partial Spectral Analysis."

Total Spectral Analysis: In the first class of inputs, the amplitude spectrum for the entire spectrum (i.e., it contains both the deterministic and non-deterministic components of the frequency spectrum) is entered into the code. The phase angles for the deterministic components are included in the input data. The phase angles for the non-deterministic components are not defined in the input. An algorithm examines the input data to determine if an associated phase angle is included for each amplitude. If a phase angle is included, the code will use that phase angle. If a phase angle is not included, the code generates a random phase for that component of the amplitude spectrum. Thus, the FFT and associated algorithms form the synthesized time series given by:

$$\sigma_j(t_k) = FFT^{-1}\left[A_i(r_a)_j\ ,\ \phi_i\right] \quad , \tag{1.17}$$

where $\sigma_j(t_k)$ is a discrete time series of the stress with a fixed time increment of $\Delta\tau$, defined by Equation (1.6). As described above, if ϕ_i is not defined in the input, then it will be assigned a random value. If more than one time synthesis are performed, the random value assigned to each undefined ϕ_i will be changed to a new random value between 0 and 2π.

Partial Spectral Analysis: In the second class of inputs, the amplitude spectrum is divided into its deterministic and non-deterministic components. The amplitude spectrum of the non-deterministic components and the azimuth-averaged time-series function for the deterministic components are entered into the code. The algorithm for the LIFE2 code first forms the inverse FFT for the non-deterministic components. Namely,

$$a_j(t_k) = FFT^{-1}\left[A_i(r_a)_j\ ,\ \phi_i\right] \quad . \tag{1.18}$$

Again, $a_j(t_k)$ is a discrete time series of the stress with a fixed time increment of $\Delta\tau$, defined by Equation (1.6). As this spectrum contains only the non-deterministic components, all values of ϕ_i should be undefined in the input data. They are assigned a random value by the code. If more than one time synthesis are performed, the random value assigned to each ϕ_i will be changed to a new random value.

The azimuth average time series is defined by the discrete function $A(\Phi_k)$ where Φ_k is the angular position of the blade. This function is then added to the time series synthesized from the random components, Equation (1.18). Namely,

$$\sigma_j(t_k) = A(\Phi_k) + a_j(t_k) \quad . \tag{1.19}$$

To maintain timing between the synthesized time series for the random component and the harmonic component of the off-axis bending stress, the value of Φ_k must correspond to the time interval of the synthesized time series. The relation between the two is given by

$$t_k = k\,(\Delta\tau) = \frac{\Phi_k}{\omega} \quad , \tag{1.20}$$

where ω is the rotational speed of the turbine blade.

BI-AXIAL STRESS STATES

As discussed by Sutherland [5], the load spectrum imposed upon a wind turbine blade is typically decomposed into two primary bending moments; "flap" and "edgewise" bending for horizontal axis turbines and "flat" and "lead-lag" bending for vertical axis turbines. The critical fatigue loads (stress cycles) imposed on the blade of either machine may not be on one of these axes, especially if the two bending loads are in-phase with one another. Frequency domain algorithms have been incorporated into the LIFE2 code to permit the analysis of bi-axial fatigue loads.

To determine the bi-axial stress states in a blade section, the two principal bending stresses at that blade station may be added together vectorially. Namely:

$$\sigma_\theta(t) = \rho_F\,\sigma_F(t)\,\cos(\theta) + \rho_E\,\sigma_E(t)\,\sin(\theta) \quad , \tag{2.1}$$

where σ_θ is the bending stress at time t and angle θ, σ_F is the root flapwise bending, σ_E is the root edgewise bending stress, and ρ_F and ρ_E are the geometric correction factors

defined below in Equation (2.2).* The time-domain analysis described in Equation (2.1) is the preferred technique for determining the bi-axial bending moment stresses. However, when using time-series measurements, sufficient data are typically not available and when using structural analysis techniques, the results are typically frequency-domain stress spectra. Thus, the determination of bi-axial bending stresses should also be addressed in the frequency domain.

Geometric Parameters

The angle θ is defined here to be the angle from the positive edgewise bending neutral axis toward the negative flap bending neutral axis; i.e., from the tension side of the flap bending moment to the tension side of the edgewise bending moment, see Figure 1. The geometric factors ρ_F and ρ_E adjust the bending stress at the outer fibers of the principal axes to the bending stress at the outer fibers at the angle θ. The values for ρ_F and ρ_E are determined from:

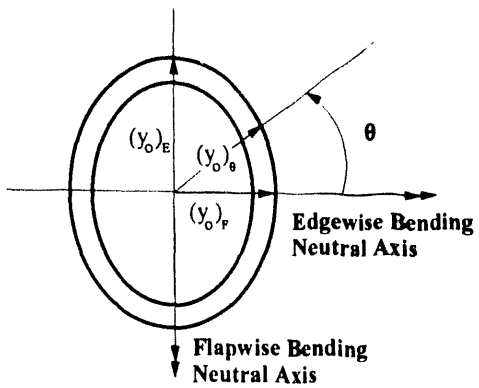

Figure 1. Geometric Parameters.

$$(\rho_F)_\theta = {(y_o)_\theta}/{(y_o)_F}$$

$$(\rho_E)_\theta = {(y_o)_\theta}/{(y_o)_E} \qquad (2.2)$$

where $(y_o)_\theta$ is the distance from the intersection of the neutral axes to the outer fibers at angle θ, and $(y_o)_F$ and $(y_o)_E$ are the distances from the neutral axis to the outer fibers along the flap and the edgewise axes, respectively (see Figure 1).

Frequency Domain Analysis

As discussed by Sutherland [5], the analysis incorporated into the LIFE2 code assumes that the harmonic components of the two bending stress states are correlated and in-phase with one another, and their random components are assumed to be uncorrelated. The algorithm incorporated into the LIFE2 code forms the time series for each component using either the analyses described in Equation (1.17) or in Equations (1.18) to (1.20).

---

* Although the flap and edgewise notation used here implies a horizontal axis turbine, this analysis is equally valid for a vertical axis turbine.

The results of this analysis are then combined using Equation (2.1) to form the synthesized time series for the bending stress at the angle θ. With the deterministic and non-deterministic components divided, the result takes the form:

$$\sigma_j(t_k) = \rho_F \left[A_F(\Phi_k) + (a_F)_j(t_k)\right]\cos(\theta) + \rho_E \left[A_E(\Phi_k) + (a_E)_j(t_k)\right]\sin(\theta) \tag{2.3}$$

NUMERICAL IMPLEMENTATION

INPUT FILES

As described in the above equations, the LIFE2 code requires the input of an amplitude spectrum with some fixed phase angles for the combined input [see Equation (1.17)] and an amplitude spectrum with no fixed phase angles and an azimuth average time history [see Equation (1.19) or (2.3)]. Both sets are input into the code in ASCII formatted files in a column format.

Typical Data

To illustrate these entries, data previously reported by Sutherland [5] and Sutherland and Osgood [6] will be used here. These data were collected by the NREL Cooperative Research Program on the NPS 100-kW turbines in Altamont Pass, California. They are described in Coleman and McNiff [10]. The NPS turbine is a two-bladed, upwind, teetering hub design utilizing full-span hydraulic passive pitch control. The fiberglass rotor blades, including the elastomeric teetering hub, span 17.8 meters (rotor diameter). The rotor's low-speed shaft turns a two-stage, two-speed gearbox. The high-speed shaft of the gearbox is connected to one of two fully enclosed induction generators. The present paper discusses data collected during operation of the turbine's 100-kW generator, which is rated at full power when rotating at 71.8 rpm in a 14 m/s wind.

Several turbine configurations were used during the collection of the NREL data set. Here, we have selected a data set for the turbine in a "locked yaw" (stiff spring) and "free teeter" with damping and stiffness. For this configuration, a 1.14-hour data segment was extracted from the main data set. During this period, the turbine was operated continuously at approximately 71.6 rpm. The average wind speed for this data set was 11.00 m/s with a turbulence factor (RMS) of 3.62 m/s.

Amplitude Spectra

The amplitude spectra is input into the code as a two column entry. The first column is the amplitude spectra and the second is the phase angle. The code assumes that the

amplitude data is at a fixed frequency increment of Δf [see Equation (1.7)]. The first entry corresponds to the "zero" frequency component, i.e., the mean value. The value of Δf is input by the operator from the keyboard. If the column does not contain an integer power of two number of entries [see Equation (1.5)], then the number of entries will automatically be increased to the next integer power of two by the code. All of the additional entries will have an amplitude of zero.

The phase angles for each amplitude is entered in the second column of the input file. If the entry for an amplitude is **blank**, the code assumes that a random phase is desired for that amplitude. If the entry is not blank, the code assumes that the phase angle for this amplitude is fixed. **All phase angles are assumed to be in units of radians.**

Note: A zero entry constitutes a fixed phase angle of zero radians. The number of entries is limited to 4096.

The two columns of data are read into the code using a "free" format. The only restriction on the entries is that the amplitude and its phase (may be blank) are on the same line and that they separated by a common delineator, e.g., a space, a comma, a semicolon, a tab, etc.

The amplitude spectrum for the flap bending stress is shown in Figure 2. The first few entries of the flap bending stress spectrum file are listed in Appendix A. The data for this spectrum contain both the deterministic and non-deterministic components. With the deterministic signal removed, the spectrum becomes that listed in Appendix B. Again, only the first few data points are listed in this Appendix. A plot of the edgewise, bending stress amplitude spectrum is shown in Figure 3.

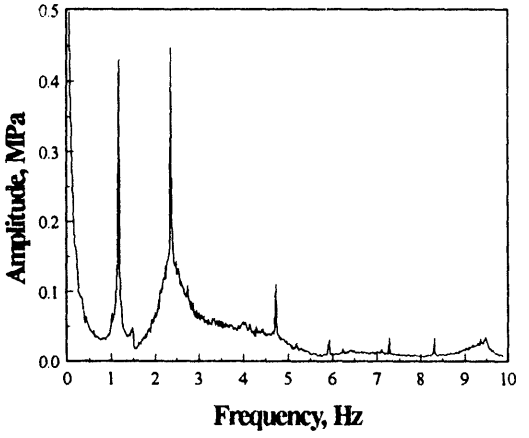

Figure 2. Amplitude Spectrum for the Root Flap Bending Stress.

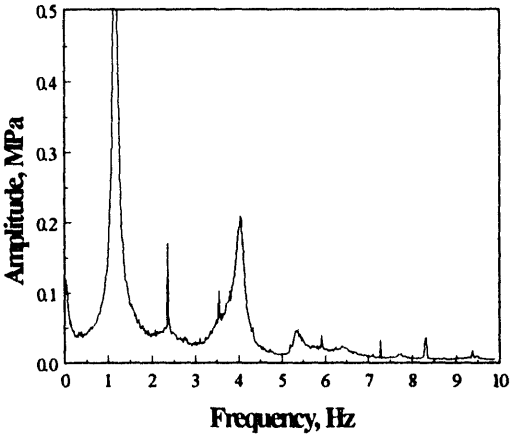

Figure 3. Amplitude Spectrum for the Root Edgewise Bending Stress.

Azimuth Average

The azimuth average data is input into the code with a single column entry. The data are spaced at a time interval $\Delta\tau$ that is defined by Equation (1.20). Each entry in this data set must be on a separate line. Any additional columns of data will be ignored by the code. The data are read into the code using a "free" format. The edgewise azimuth average data is shown in Figure 4 and are listed in Appendix C.

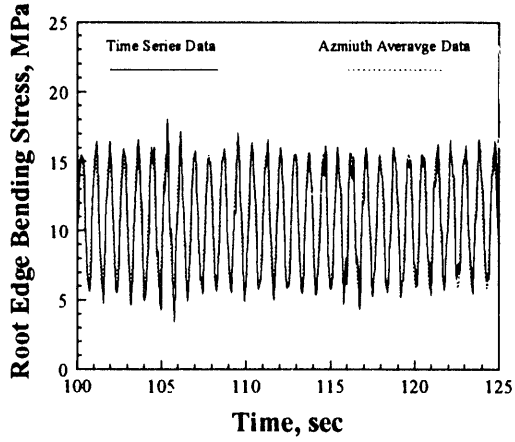

Figure 4. Typical Root Edgewise Bending Moment Stress Histogram. The solid and dashed lines overlay one another almost everywhere.

COMPUTATIONS

The LIFE2 code uses the input amplitude spectrum file(s) to synthesize time series based on the equations presented above. The resulting time series is then counted using the rainflow counter previously implemented into the code by Schluter and Sutherland [3]. The rainflow algorithm characterizes, or counts, each fatigue stress cycle (closed hysteresis loop) in the time series by its mean value and its **peak-to-peak** range or its amplitude (half range)* . Post processing algorithms contained in the code "bins" each cycle by these values in a cycle count matrix that is used in the prediction of service lifetime by the code [1].

INTERIM CYCLE COUNTS

The operator is asked by the code for the number of times the spectral data should be used to synthesize time series data. Each synthesis produces a time series of T seconds long {see Equation (1.7)]. If a large number of these syntheses are to be processed by the code (see the discussion below) then the computer's storage will be filled to capacity, causing an internal computational error that will terminate the program. To insure minimum disruption from this storage problem, the code synthesizes the frequency spectrum in groups of ten. The resulting time series are written "back-to-back" in a single file and then the rainflow counter performs an interim cycle count that converts this time series information into a cycle count matrix. The code then processes another group of ten time series syntheses. The previous time series information is overwritten by the new time series, thus limiting the quantity of hard disk space required to perform these functions.

* Starting with version 3.06 of the LIFE2 code, the rainflow counter may be set to count stress cycles in terms of their range (peak-to-peak) or their amplitude (half range).

The rainflow counter then performs another interim count, and adds the current cycle counts to the previous cycle count matrix. In this manner the code progresses through the synthesis process to the number required.

STABLE SOLUTIONS

As discussed above, the algorithms presented here, and incorporated into the LIFE2 code, use an FFT to convert frequency spectra to time series and then a rainflow counter to convert the time series to cycle counts. This technique is relatively robust, in that it is able to successfully process a wide variety of data. And, with fixed phase angles, the technique provides a unique solution which can be obtained with a single synthesis. However, the use of random phase angles requires that a relatively large number of time series must be synthesized to obtain a "stable" answer. Here, the term "stable" implies that the cycle count matrix that results from the synthesis process contains a stable distribution of cycle counts. When normalized, the distribution of cycle counts does not change significantly when additional synthesis data are added to it; the distribution is relatively smooth, and its high-stress tail is a monotonically decreasing distribution of the cycle counts. As discussed by several authors [4, 5, 6, 11, 12 & 13], the cycle counts should converge to a relatively smooth distribution as time lengths are increased. Moreover, the population of cycle counts in the high-stress tail on the cycle count distribution is very important in the determination of the service lifetime of a turbine component, because a significant portion of the damage to the turbine is concentrated in this high-stress tail. **Thus, the operator must be extremely sensitive to both the number of synthesized time series and the form of the cycle count matrix to insure that the synthesis process has produced a stable result.**

The progression of the cycle count distribution to a stable solution is shown for a typical example in Figure 5. These data were synthesized from the edgewise frequency spectrum shown in Figure 3. In this figure, the number of cycle counts has been normalized to 100 seconds to permit direct comparisons of the distributions. As observed in this Figure 5, the distribution is bi-modal. For relatively short synthesis times, Figure 5a and 5b, the cycle counts do not have a smooth distribution. Rather, the distribution contains gaps, and the high stress tail of the distribution (the stress bins that are greater than approximately 17 MPa) does not decrease monotonically. As the synthesis time increases, see Figure 5c and 5d, the gaps are filled and the distributions becomes smoother. The final distribution, Figure 5d, is not completely smooth. It contains gaps in the 23 and 24 MPa bins and it is not monotonically decreasing above approximately 22 MPa. However, the essence of the distribution has been captured and these relative minor variations do not change, significantly, the damage predicted for this distribution. If they did, additional frequency synthesis data could be added to this distribution to further smooth it.

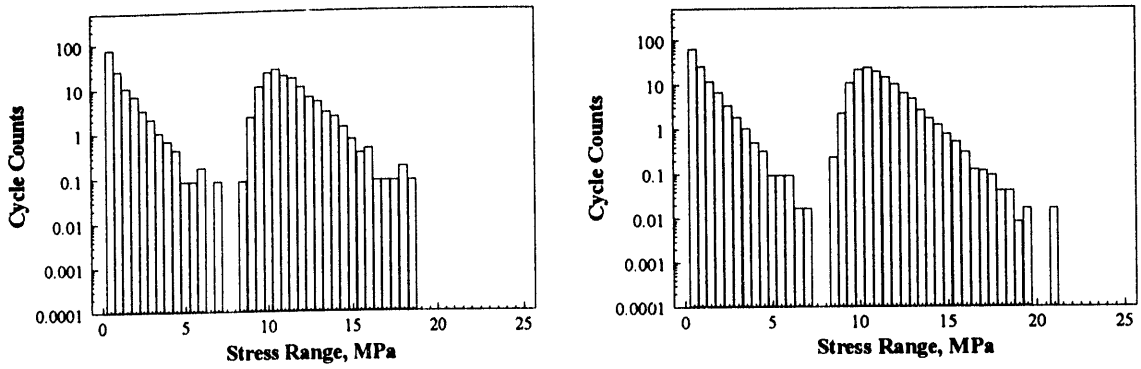

a. 120 Seconds

b. 1200 Seconds

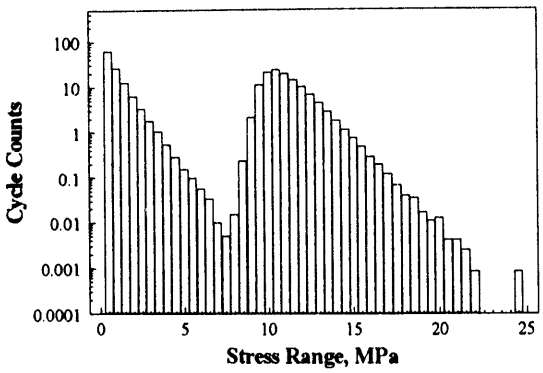

c. 12000 Seconds

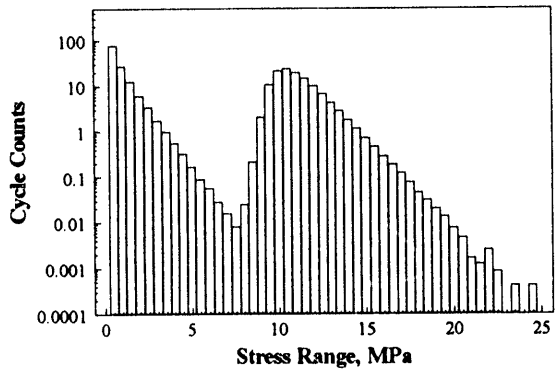

d. 24000 Seconds

Figure 5. Progression to a Stable Solution. Data Normalized to 100 Seconds.

Examination of Cycle Count Distribution

To achieve a stable solution typically requires the synthesis of a very large number of time series. As discussed below, the computations can be speeded, somewhat, through a judicious selection of operating environments. However, the operator is the ultimate authority to determine when a solution has become stable. The LIFE2 code does provide the operator with an aid to evaluating the stability of a cycle count synthesis. In particular, the LIFE2 code is able to plot the cycle counts directly to the computer's display (see the discussion of the plotting capabilities of the code, below).

The plots provided by LIFE2 code include a three-dimensional (3D) plot of the cycle counts (cycle counts vs mean and alternating stress). Also provided are two-dimensional (2D) plots of cycles counts vs either mean or alternating stress. For the former 2D plot,

the cycle counts at a given mean stress are summed over all alternating stresses, and in the latter they are summed over all mean stresses. The 2D plots are the most useful in examining the stability of a solution.

Example

A sample of the plots produced by the LIFE2 code are shown below for the sample problem. Rather then reproduce these plots in this section, we will use enhanced versions of the 2D plots, from Sutherland and Osgood [6], to illustrate the stability of the solution. For the flap bending stresses in the NPS turbine, the plots of the cycle counts are shown in Figures 6 and 7. Also included in these plots are cycle counts taken directly from the measured time series data. Note that the number of cycle counts has been normalized to 100 seconds in these plots. This normalization permits the direct comparisons of cycle counts for time series of different lengths.

As shown in these two figures and in Figure 5, over 240,000 seconds (66 hours) of synthesized time series data were required to achieve a stable and relatively smooth distribution of cycle counts in the high-stress tail. As each synthesis produced a time series 51.2 seconds in length, the information summarized in these two figures required the frequency spectrum be processed over 4000 times.

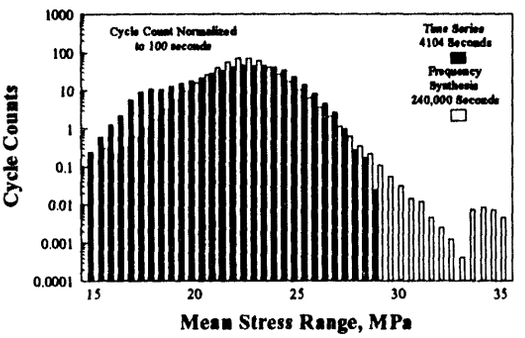

Figure 6. Mean Stress Cycle Count Distribution for Measured Data and Synthesized Time Series Data, Root Flap Bending Stress.

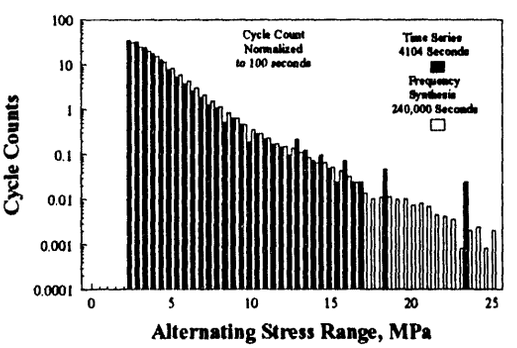

Figure 7. Alternating Stress Cycle Count Distribution for Measured Data and Synthesized Time Series Data, Root Flap Bending Stress.

The comparison of the synthesized time series data with the time series data shown in these two figures illustrates that the spectral technique predicts more cycles in the high-stress tail of the distribution. The relatively smooth distribution of cycle counts in this high-stress tail is indicative of the relatively long time series, over 240,000 seconds, synthesized for this analysis. As discussed in References 4, 5, 6, 11, 12 and 13, the cycle counts from time series data should converge to a relatively smooth distribution as time lengths are increased. The relatively disjoint distribution shown in Figures 6 and 7 are a

direct result of the relatively short duration (4004 seconds compared with 240,000 seconds) of the time series data. Thus, the distribution and magnitudes of the cycle counts are in excellent agreement with the cycle counts obtained directly from the time series data. However, a very long synthesis process is required to obtain this information.

Comments on Stability

In summary, the operator must be prepared to conduct the synthesis process many times before a stable answer is achieved. To follow the progress toward a stable answer, the operator may use the plotting capabilities of the code to follow the stress cycles in the high stress tail of the distribution.

SPEEDING OPERATIONS

The use of the LIFE2 code to synthesize time series from frequency spectra and to cycle count that result is a computationally intensive operation. To speed the operation of this numerical analysis, the authors suggest that the LIFE2 code be the only program running during this operation, i.e., the code has top priority and no background program(s) is allowed. All TSRs should be closed. Further, operations can be greatly speeded by executing the LIFE2 code from a RAM disk rather than a hard disk. Avoid running the code over a network or to any other relatively slow storage device. In the RAM mode, the operator must be sure to save the final computations to permanent media, because the RAM data will be lost when the computer is turned off.

Needless to say, the faster the processor, the faster the solution. However, the operator should remember that the LIFE2 code is a PC based code. Even with the fastest processors now available, the synthesis of the data summarized in Figures 5 and 6 will require several days of computations.

FILES

The files used by the frequency domain analysis are listed in Appendix D. This list of files also contains a brief description of the information contained in each file. As noted in the appendix, the files with either a "dat" or a "tmp" extension should be deleted after the completion of a synthesis procedure.

EXAMPLE SESSION WITH TYPICAL RESULTS

This volume is the fifth in a series of Reference/User's Manuals for the LIFE2 code. The other 4 volumes are listed as References 14, 15, 16 and 17. This section of the paper assumes that the reader has the other volumes available for reference.

DOCUMENTING UNITS

The LIFE2 code is unit insensitive. The user must assure that compatible units are used throughout the calculation. The code will ask for the units being used in the calculation so that they may be documented in the data files. As this module uses the rainflow algorithm already contained in the LIFE2 code, the output of the computational module will produce rainflow counts based on either the **RANGE** (peak-to-peak) or the **AMPLITUDE** (half range) of the stress cycle.

OPERATOR INPUTS

The following is an example session using the rainflow counting algorithms with the data files cited above.

In the example, LIFE2 code prompts are written in **bold letters**. The operator's responses to the prompts are written in *italics*. The frequency spectra files used in this example are shown in Appendices A, B and C. These are very simple files and are meant for illustrative purposes.

Access

Starting at the Main Menu, the frequency synthesis is accessed via the Stress State Module. The current version of the LIFE2 code is 3.06.

LIFE2 -- Version 3.06

>>> Main Menu <<<

The options at this level are

1) Enter the Wind Spectrum
2) Enter the Constitutive Properties
3) Enter the Stress States
4) Enter the Operational Parameters
5) Calculate the Life of a WECS Component

9) Exit Life2 Code

Enter the number of the desired option.>*3*

Then, for any of the three classes of Stress States:

>>> Stress State Menu <<<

This menu allows the operator to select which type of stress matrix to input.

The options at this level are

1) Enter Operational Stresses
2) Enter Buffeting Stresses
3) Enter Start/Stop Stresses

9) Return to Main Menu

Enter the number of the desired option.> *1*

Select Rainflow Counting:

>>> Operational Stresses Menu <<<

This option allows the operator to input the operational stresses for a wind turbine.

The current Operational Stress Data Base in operational memory is Calculational file does not exist!

The options at this level are

1) Retrieve data from the Operational Stresses Library
2) Input Tabular Operational Stress Data
3) Calculate New Operational Stress Data
4) Rainflow Count a Data File
5) Plot an Operational Stress Data File
6) Change Units of Wind Speed and/or Stress
7) Add a Data File to the Operational Stresses Library
8) Delete a Data File from the Operational Stresses Library

9) Return to the Stress State Menu

Enter the number of the desired option.> *4*

and, the Frequency Spectrum analysis module:

The options at this level are
1) Rainflow Count a Time Series Data File
2) Rainflow Count from a Frequency Spectrum

9) Return to the Previous Menu

Enter the number of the desired option.> *2*

At this point, the operator is ready to start the frequency domain analysis procedure.

Frequency Domain Analysis

Input Data: For the example problem cited above, the full frequency spectra for the flap and edgewise bending stresses are assumed to be in the npsflp.ffq and the npsedg.ffq files, respectively. The non-deterministic frequency spectra are the npsflp.rfq and the npsedg.rfq files. The azimuth average signals are in the npsflp.azm and npsedg.azm files. The frequency step in each file is 0.017578. The units of stress are MPa.

Data Entry: To start a new file, select 1. To add data to an existing file select 2. Here, we will assume the former.

The options at this level are:
1) Input Frequency Data into a New Cycle Count File
2) Add Frequency Data to an Existing Cycle Count File

9) Return to the Operational Stress Menu

Enter the number of the desired option.> *1*

Input the requested data.

Enter the title of the data set no longer than 72 characters.
Example for user's guide. NPS Flap Data. Total Spectral Analysis.

Enter the units of stress no longer than 20 characters.
MPa

The operator may choose to characterize the cycle counts by either their range or their amplitude. Here, we will use range.

The RANGE of the Alternating Stress is the difference between the maximum and minimum (i.e., peak to peak) stress.

The AMPLITUDE (or half Range) of the Alternating Stress is the difference between the maximum and minimum (i.e., peak to peak) stress divided by two (2).

The Material Properties and the Cycle Count Matrices both must be RANGE Variables or both must be AMPLITUDE (half Range) Variables.

Do you wish the Alternating Stress to be defined as:

1) An AMPLITUDE Variable
2) A RANGE Variable

Enter the number of the desired option.>*2*

Enter the units of wind speed no longer than 20 characters.
m/s

The next two inputs define the operational wind speed bin associated with this set of calculations.

Input the lower range of the wind speed.>*9*
Input the upper range of the wind speed.>*11*

i.e., the file being transformed here is based on information gathered between 9 and 11 meters per second (m/s).

For the full frequency spectrum, input the following:

Input the name of the file that contains the frequency spectrum.
npsflp.ffq

What is the frequency increment for these data?
0.017578

Is a deterministic file to be added to the frequency data?(Y or N)
n

For the non-deterministic frequency spectrum added to the azimuth average the inputs differ as follows:

Input the name of the file that contains the frequency spectrum.
npsflp.rfq

What is the frequency increment for these data?
0.017578

Is a deterministic file to be added to the frequency data?(Y or N)
y

What is the name of the file containing the deterministic signal?
npsflp.azm

The code then presents the mean stress value (the first entry in the frequency spectrum) to the operator. The operator is offered the opportunity to change it at this point.*

The mean value of the amplitude is -.1090 MPa

Would you like to change this value?(Y or N)
n

The stress then can be moved to the outer fiber based on the geometric factor defined in Equation (2.2). An input of one (1) leaves the data unchanged. If this question is answered no, the default value assumed by the code is one. Here, a value of 1 is entered for illustrative purposes.

Is the frequency file to be multiplied by a geometric factor?(Y or N)
y

Please enter the geometric factor.
1

For the analysis of a single axis of information, the answer to the next question is no.

Is another frequency file to be added to the first at an off angle?
(Y or N)
n

For the analysis of a bi-axial case, the answer to the question is yes.

Is another frequency file to be added to the first at an off angle?
(Y or N)
y

* In many FFTs, the first term in the Fourier Transform is set to zero to speed computations. The ability to change this value at this point in the operation of the code is provided to handle these cases.

The operator will then be asked for the following information. Note that these questions are identical to the information provided by the operator for the first file. The operator is not prompted for the frequency increment in this case because it must be the same in both input frequency spectra. **The "angle" between the bending axes is defined in Figure 1 and in Equations (2.1) through (2.3). Figure 1 is based on the assumption that the flap bending stress spectra is entered into the code as the first data set and the edgewise bending stress spectra is entered as the second data set.** This angle may be positive or negative, and it is assumed to be in degrees.

What is the name of the second frequency file?
npsedg.rfq

What is the phase angle between the two frequency files?
(in degrees)
45

Is a deterministic file to be added to the frequency data?(Y or N)
y

What is the name of the file containing the deterministic signal?
npsedg.azm

The mean value of the amplitude is -.0093 MPa

Would you like to change this value?(Y or N)
n

Is the frequency file to be multiplied by a geometric factor?(Y or N)
n

The operator is then asked to define the variation in the standard deviation in the input, i.e., R_a and the number of increments, J, as defined in Equation (1.9).

Would you like to vary the standard deviation of the input frequency spectrum?(Y or N)
y

The standard deviation of the input frequency will be varied about its mean.

Please input the fractional variation desired for this input frequency spectrum.
0.5

How many steps do you want in the variation of the standard deviation of the input frequency spectrum?
10

The operator is asked the total number of times the input files are to be processed. See the above discussion concerning the stability of the solution using this technique. Note that the total number of synthesized time series should be an even multiple of the variable J, defined in the above input.

How many times do you want the input file processed?
This number must be a multiple of the number of steps per interval, which is 10.
20

The operator is then prompted with the standard inputs for the rainflow counter. See References 16 and 17 for complete definitions of these inputs.

Do you want to find the peaks and valleys in the data?(Y or N).>*y*

Input the threshold value.
0.1

For the first use of the frequency spectrum analysis, the code will ask the operator for an integer number. This is the "seed" for the random number (phase) generator. After the first input, the seed will automatically be undated and recorded by the code.

Please enter a number between 0 and 2147483647.
92398643

The code details the statistics from the first ten time series that are synthesized and asks the operator to define the size of the cycle count bins.

The extreme values for the mean stress are

Minimum = 16.34731000

Maximum = 29.39874000

Input the desired resolution for the mean stress intervals.
0.5

The extreme values for the alternating stress are

Minimum = .10083960

Maximum = 17.50374000

Input the desired resolution for the alternating stress intervals.
0.5

This completes the entries for this series of calculations. The statistics for the last ten synthesized time series and the input frequency spectra are listed for the operator. Note which variables are and are not included in the formulation of these statistics.

	Frequency Spectrum Statistics (deterministic series not included) (variation in std. dev. not included)	Time Series Statistics (deterministic series included) (variation in std. dev. included)
Minimum =	- .16	14.53
Maximum =	1.90	33.52
Mean Value =	- .11	23.19
Standard Deviation =	1.42	3.02

Press return to continue.

Is another time series to be entered into this file?(Y or N)>*n*

At this juncture, the operator may continue with the calculations or conclude the operation of the code. If the operator concludes the current operation, notes may be added or updated [14].

Enter the number of miscellaneous notes for this data set.>*1*

Enter note 1 no longer than 72 characters.
Operator: HJS

The operator is offered the chance to archive this information via the library functions described in Reference 14.

Do you wish to store the new data?(Y or N)>*y*

The following is a list of data files currently available in the library:

Enter a 1-6 character name under which to store the file just created, revised, or added.>*exampl*

This concludes the operational inputs for this section of the code.

Plotting the Results

To plot the data generated by this or any other stress state modules, return to the operational, buffeting, or start/stop stress state menu and choose option 5. For the "Operational Stresses Menu," the following is displayed. Note that the previous NPS calculations have been retrieved from the code's archived files [14], for this section of the paper. The data used here is the NPS data cited above to synthesis bi-axial data at a $+45^{o}$ angle. Two values of R_a were used: the first was 0.5 and the second was 1.1. For the former, ten steps were used; for the latter, one step was used. A complete description of these synthesized data is provide in Reference 5.

>>> Operational Stresses Menu <<<

This option allows the operator to input the operational stresses for a wind turbine.

The current Operational Stress Data Base in operational memory is
NPS Data Analysis; Ch 2 & 3 @ +45deg w/ Amp @.5 S@1.1;FreSp 7/24/92
The stress units for this file are: MPa
The wind speed units for this file are: m/s

The options at this level are

1) Retrieve data from the Operational Stresses Library
2) Input Tabular Operational Stress Data
3) Calculate New Operational Stress Data
4) Rainflow Count a Data File
5) Plot an Operational Stress Data File
6) Change Units of Wind Speed and/or Stress
7) Add a Data File to the Operational Stresses Library
8) Delete a Data File from the Operational Stresses Library

9) Return to the Stress State Menu

Enter the number of the desired option.> *5*

This choice yields the library query [14],

Is the data to be plotted in the current ops.cal file?
y

The intervals in the current calculations are then listed and may be plotted.

```
The total number of intervals:  1


 1)  Operational Stresses; # Records =4000;  Range  9.00 to 11.00


Options:
      F - Page Forward      B - Page Backward
      P - Plot Interval     E - Exit

Enter the desired option.>p

What is the interval number to be plotted?
1
```

The plot menu is then displayed.

```
                >>>Stress Plotting Menu<<<

The options at this level are:

  1) Change Plot Parameters
  2) 2d-Plot of Alternating Stresses
  3) 2d-Plot of Mean Stresses
  4) 3d-Plot of Mean and Alternating Stresses

  9) Return to Operational Stresses Menu

Enter the number of the desired option.>2
```

At this point, the operator may set/change the current hardware configuration (a default configuration is loaded for the first set of plots; thereafter, any updates in the configuration is archived by the code), or plot the data. A summary of the default setup and a complete list of the various hardware configurations are provided in Appendices E and F, respectively.

Three separate plots of the cycle count matrix are available: the first is a 2-D plot of the alternating stresses summed over all mean stresses (see Figure 8), the second is a 2-D plot of the mean stresses summed over all alternating stresses (see Figure 9), and the third is a 3-D plot of the cycle counts (see Figure 10). After prompts concerning the display format, see Reference 14, the plot will be shown on the computer display.

```
 Would you like the plot to be semi-logarithmic? (Y/N)
y


 .....Plotting
```

The operator is queried for the display.

READY TO DISPLAY DRAWING.
Strike any key to continue.

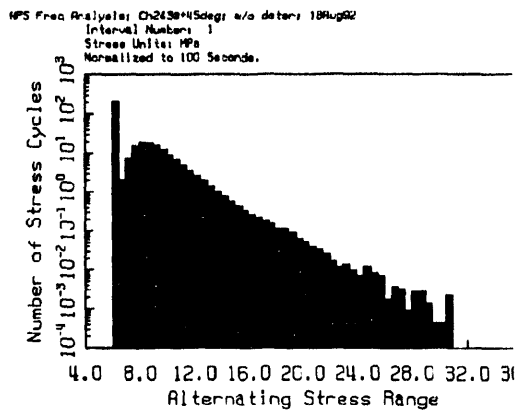

Figure 8. Alternating Stress Cycle Count Distribution for Synthesized Time Series Data at Positive 45 Degrees.

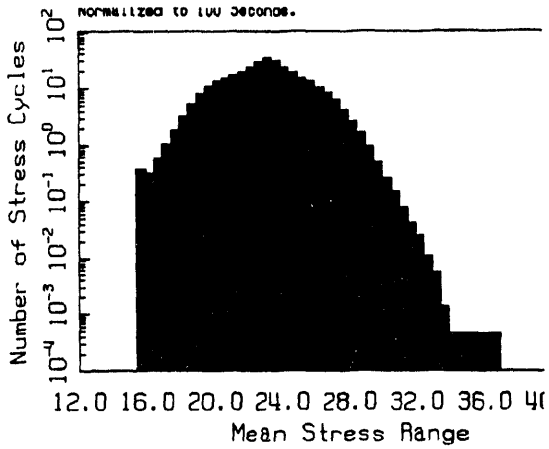

Figure 9. Mean Stress Cycle Count Distribution for Synthesized Time Series Data at Positive 45 Degrees.

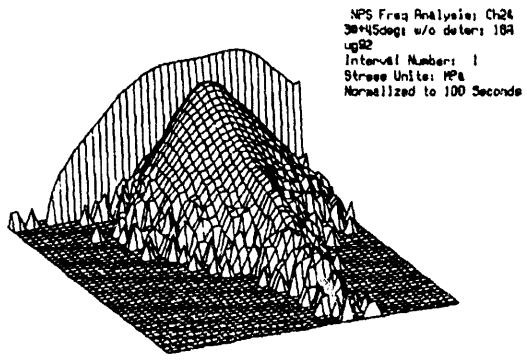

Figure 10. Cycle Count Distribution for Synthesized Time Series Data at Positive 45 Degrees.

Following this display, the operator is queried to determined if the plot should be sent to a printer.

```
Would you like a hard copy of the plot? (Y/N)
n
```

The operator is then returned to the plotting menu.

The typical plots shown in Figures 8, 9 and 10 are for approximately 4000 synthesized sets of time series data at a positive 45° angle. These plots were produced by the code on a Laserjet printer.

CONCLUDING REMARKS

The LIFE2 computer code is a fatigue/fracture code for the analysis of wind turbine components. The computational modules described in the paper permit frequency-domain stress spectra to be cycle counted. The algorithm uses a Fourier analysis to transform frequency-domain spectra to an equivalent time series suitable for rainflow counting by other modules in the code. This paper describes the algorithms incorporated into the code and, their numerical implementation. Example problems are used to illustrate typical inputs and outputs.

REFERENCES

1. Sutherland, H. J., and L. L. Schluter, "The LIFE2 Computer Code, Numerical Formulation and Input Parameters," *Proceedings of WindPower '89*, SERI/TP-257-3628, September 1989, pp. 37-42.

2. Akins, R. E., Rainflow Counting Based on Predicted Stress Spectra, Presented at the *Eighth ASME Wind Energy Symposium*, Houston, 1989.

3. Schluter, L. L., and H. J. Sutherland, "Rainflow Counting Algorithm for the LIFE2 Fatigue Analysis Code," *Proceedings of the Ninth ASME Wind Energy Symposium*, D. E. Berg (ed), SED-Vol. 9, ASME, January 1990, pp. 121-123.

4. Sutherland, H. J., "Frequency-Domain Stress Prediction Algorithm for the LIFE2 Fatigue Analysis Code," *Proceedings of the Eleventh ASME Wind Energy Symposium*, P. S Veers and S. Hock (eds), SED-Vol. 11, ASME, January 1992, pp. 107-113.

5. Sutherland, H. J., "Effect of the Flap and Edgewise Bending Moment Phase Relationships on the Fatigue Loads of a Typical HAWT," *Wind Energy - 1993*, S. Hock (ed), SED-Vol. 14, ASME, January-February 1993, pp. 181-187.

6. Sutherland, H. J., and R. M. Osgood, "Frequency-Domain Synthesis of the Fatigue Load Spectrum for the NPS 100-kW Wind Turbine," *Proceedings of WindPower '92*, AWEA, Washington, DC, October 1992, pp. 321-328.

7. Ramirez, R. W., *The FFT, Fundamentals and Concepts*, Prentice Hall, Englewood, 1985.

7. Jones, R. E., *FFT Subroutines, Sandia Mathematical Program Library*, Ver. 8.1, Albuquerque, 1980, (based on the algorithms developed by N. M. Brenner, MIT Lincoln Lab, and Cooley, Lewis and Welsh, IBM).

9. Jones, R. E., *Random Number Generator, Sandia Mathematical Program Library*, Albuquerque, 1980.

10. Coleman, C., and B. McNiff, *Final Report: Dynamic Response Testing of the Northwind 100 Wind Turbine*, Subcontractor Report, SERI Cooperative Research Agreement #DE-FC02-86CH10311, Solar Energy Research Institute, Golden, CO, 1989, 40 pp.

11. Veers, P. S., "Simplified Fatigue Damage and Crack Growth Calculations for Wind Turbines," *Proceedings of the Eight ASME Wind Energy Symposium*, D. E. Berg and P. C. Klimas (eds), SED-Vol. 7, ASME, January 1989, pp. 133-140.

12. Thresher, R. W., S. M. Hock and R. M. Osgood, "Data Record Length Effects on Rainflow Analysis," *Proceedings of the Eleventh ASME Wind Energy Symposium*, P. S. Veers and S. Hock (eds), SED-Vol. 11, ASME, January 1992, p. 117.

13. Malcolm, D. J., "Predictions of Peak Fatigue Stresses in a Darrieus Rotor Wind Turbine Under Turbulent Winds," *Proceedings of the Ninth ASME Wind Energy Symposium*, D. E. Berg (ed), SED-Vol. 9, ASME, January 1990, pp. 125-135.

14. Schluter, L. L., and H. J. Sutherland, *Reference Manual for the LIFE2 Computer Code*, SAND89-1396, Sandia National Laboratories, Albuquerque, NM, September 1989, 170 p.

15. Sutherland, H. J., *Analytical Framework for the LIFE2 Computer Code*, SAND89-1397, Sandia National Laboratories, Albuquerque, NM, September 1989, 42 p.

16. Schluter, L. L., and H. J. Sutherland, *User's Guide for LIFE2's Rainflow Counting Algorithm*, SAND90-2259, Sandia National Laboratories, Albuquerque, NM, January 1991, 37 p.

17. Schluter, L. L, *Programmers Guide for LIFE2's Rainflow Counting Algorithm*, SAND90-2260, Sandia National Laboratories, Albuquerque, NM, January 1991, 30 p.

APPENDIX A

The Total Spectrum for Flap Bending Stress

NPS 100-kW Wind Turbine

The data contained in this file is the amplitude spectrum for the flap bending stress of the NPS 100-kW turbines in Altamont Pass, California. The file is called npsflp.ffq in the example cited above. Only the first 144 entries are reproduced here. To save space and increase the readability of these data, the file has been "wrapped" into four columns. As one can note from this input, a comma is used as the delineator and only very few entries have fixed phases. A comparison of these data with Figure 2 illustrates that these fixed phases are associated with the peaks in the amplitude spectrum.

column 1	column 2	column 1 (cont.)	column 2 (cont.)
.22033E+02 ,		.43568E-01 ,	
.12127E+01 ,		.42175E-01 ,	
.77048E+00 ,		.39936E-01 ,	
.62269E+00 ,	.39385E+01	.44700E-01 ,	
.49664E+00 ,	.41403E+01	.35948E-01 ,	
.38949E+00 ,	.45010E+01	.38494E-01 ,	
.36563E+00 ,		.34899E-01 ,	
.26789E+00 ,		.36462E-01 ,	
.26690E+00 ,		.35046E-01 ,	
.21861E+00 ,		.34590E-01 ,	
.19348E+00 ,		.31886E-01 ,	
.16689E+00 ,		.32251E-01 ,	
.16378E+00 ,		.31140E-01 ,	
.15455E+00 ,		.31071E-01 ,	
.13968E+00 ,		.32788E-01 ,	
.12423E+00 ,		.33051E-01 ,	
.10083E+00 ,		.31841E-01 ,	
.96300E-01 ,		.33744E-01 ,	
.91784E-01 ,		.31893E-01 ,	
.92825E-01 ,		.31106E-01 ,	
.88393E-01 ,		.34688E-01 ,	
.75695E-01 ,		.35373E-01 ,	
.68135E-01 ,		.37022E-01 ,	
.65697E-01 ,		.39198E-01 ,	
.54986E-01 ,		.37851E-01 ,	
.64698E-01 ,		.44738E-01 ,	
.60270E-01 ,		.51629E-01 ,	
.53581E-01 ,		.69024E-01 ,	
.53218E-01 ,		.55929E-01 ,	
.51082E-01 ,		.62370E-01 ,	
.46221E-01 ,		.62822E-01 ,	
.45927E-01 ,		.80650E-01 ,	

column 1 (cont.)	column 2 (cont.)
.87643E-01 ,	
.11418E+00 ,	
.14421E+00 ,	
.39374E+00 ,	
.43059E+00 ,	.46545E+01
.14760E+00 ,	.42872E+01
.91354E-01 ,	
.74458E-01 ,	
.58431E-01 ,	
.48464E-01 ,	
.46582E-01 ,	
.45543E-01 ,	
.40682E-01 ,	
.37417E-01 ,	
.35490E-01 ,	
.35590E-01 ,	
.37136E-01 ,	
.39226E-01 ,	
.36263E-01 ,	
.44392E-01 ,	
.42056E-01 ,	
.48168E-01 ,	
.38503E-01 ,	
.24220E-01 ,	
.18595E-01 ,	
.19341E-01 ,	
.17514E-01 ,	
.20500E-01 ,	
.21426E-01 ,	
.22235E-01 ,	
.27065E-01 ,	
.25851E-01 ,	
.24425E-01 ,	
.31770E-01 ,	
.30286E-01 ,	
.34997E-01 ,	
.33696E-01 ,	
.33399E-01 ,	
.39043E-01 ,	
.33445E-01 ,	

column 1 (cont.)	column 2 (cont.)
.40669E-01 ,	
.44559E-01 ,	
.45970E-01 ,	
.47273E-01 ,	
.41728E-01 ,	
.51490E-01 ,	
.58103E-01 ,	
.60468E-01 ,	
.55218E-01 ,	
.58380E-01 ,	
.69765E-01 ,	
.66293E-01 ,	
.62385E-01 ,	
.73208E-01 ,	
.75578E-01 ,	
.88154E-01 ,	
.74502E-01 ,	
.95497E-01 ,	
.10448E+00 ,	
.98741E-01 ,	
.10693E+00 ,	
.11674E+00 ,	
.11913E+00 ,	
.11771E+00 ,	
.13611E+00 ,	
.11864E+00 ,	
.14209E+00 ,	
.14624E+00 ,	
.15068E+00 ,	
.15577E+00 ,	
.16507E+00 ,	.34167E+01
.44768E+00 ,	.27897E+00
.20075E+00 ,	.58293E+01
.18036E+00 ,	
.16635E+00 ,	
.14240E+00 ,	
.13828E+00 ,	
.13658E+00 ,	
.14297E+00 ,	
.12450E+00 ,	

APPENDIX B

THE NON-DETERMINISTIC SPECTRUM FOR FLAP BENDING STRESS

NPS 100-kW Wind Turbine

The data contained in this file is the amplitude spectrum for the edgewise bending stress of the NPS 100-kW turbines in Altamont Pass, California. This spectrum is different from that shown in Appendix A in that this spectrum contains only the non-deterministic portion of the bending stresses. The file is called npsedg.rfq in the example cited above. Only the first 66 entries are reproduced here. As one can note from this input, no entries have fixed phases. The deterministic signal (azimuth average) is shown in Appendix C.

column 1	column 2	column 1 (cont.)	column 2 (cont.)
-.10898E+00 ,		.41238E-01 ,	
.12694E+01 ,		.40205E-01 ,	
.79516E+00 ,		.45150E-01 ,	
.65611E+00 ,		.35744E-01 ,	
.49945E+00 ,		.41505E-01 ,	
.39612E+00 ,		.35740E-01 ,	
.36920E+00 ,		.35056E-01 ,	
.27369E+00 ,		.36592E-01 ,	
.25023E+00 ,		.33347E-01 ,	
.21721E+00 ,		.28251E-01 ,	
.19969E+00 ,		.32414E-01 ,	
.17658E+00 ,		.30138E-01 ,	
.16139E+00 ,		.28991E-01 ,	
.15836E+00 ,		.31711E-01 ,	
.14269E+00 ,		.32049E-01 ,	
.11836E+00 ,		.28840E-01 ,	
.10415E+00 ,		.32943E-01 ,	
.10170E+00 ,		.30006E-01 ,	
.90890E-01 ,		.28521E-01 ,	
.96230E-01 ,		.32969E-01 ,	
.89742E-01 ,		.33671E-01 ,	
.79653E-01 ,		.35332E-01 ,	
.67430E-01 ,		.34449E-01 ,	
.63637E-01 ,		.32300E-01 ,	
.54566E-01 ,		.42404E-01 ,	
.63442E-01 ,		.50314E-01 ,	
.59365E-01 ,		.62774E-01 ,	
.48043E-01 ,		.49535E-01 ,	
.51615E-01 ,		.52367E-01 ,	
.53666E-01 ,		.53653E-01 ,	
.44028E-01 ,		.64072E-01 ,	
.46559E-01 ,		.68676E-01 ,	
.44419E-01 ,		.88987E-01 ,	

APPENDIX C

THE AZIMUTH AVERAGE EDGEWISE COMPONENT

NPS 100-kW Wind Turbine

The data contained in this file is the deterministic (azimuth average) data for the edgewise bending stress of the NPS 100-kW turbines in Altamont Pass, California. This data is the deterministic portion of the bending stresses that was subtracted from the edgewise spectrum shown in Appendix B. The file is called npsedg.azm in the example cited above. The second column in this data, ignored by code, is the blade position in degrees.

column 1	column 2	column 1 (cont.)	column 2 (cont.)
.761823E+01 ,	.000000E+00	.141131E+02 ,	.180000E+03
.840782E+01 ,	.120000E+02	.133376E+02 ,	.192000E+03
.943407E+01 ,	.240000E+02	.124553E+02 ,	.204000E+03
.104796E+02 ,	.360000E+02	.115249E+02 ,	.216000E+03
.115444E+02 ,	.480000E+02	.105459E+02 ,	.228000E+03
.124759E+02 ,	.600000E+02	.964229E+01 ,	.240000E+03
.133567E+02 ,	.720000E+02	.875517E+01 ,	.252000E+03
.141182E+02 ,	.840000E+02	.787032E+01 ,	.264000E+03
.147539E+02 ,	.960000E+02	.711091E+01 ,	.276000E+03
.152632E+02 ,	.108000E+03	.647863E+01 ,	.288000E+03
.154641E+02 ,	.120000E+03	.614460E+01 ,	.300000E+03
.155709E+02 ,	.132000E+03	.590780E+01 ,	.312000E+03
.155107E+02 ,	.144000E+03	.587142E+01 ,	.324000E+03
.152591E+02 ,	.156000E+03	.608318E+01 ,	.336000E+03
.148153E+02 ,	.168000E+03	.654894E+01 ,	.348000E+03

APPENDIX D

THE FREQUENCY AND RAINFLOW DATA FILES

The LIFE2 code generates a set of files specific to the frequency domain analysis and the rainflow counter. This appendix provides a list of the files and a brief description of the information contained in each. Other files used by the code are described in the other reference manuals, [14, 15, 16 and 17]. All of the files with a "dat" or "tmp" extension may be deleted after an analysis is complete.

extrema.dat - Contains the Extrema (Maximum & Minimum) for Rainflow Counting.

filtered.dat - Contains the Extrema with "Small Cycles" Removed.

rain.dat - Contains the Mean and Stress Amplitude for the RainFlow Counting.

tfq.dat - Contains the Time Series Data Synthesized by the Frequency Spectrum Analysis.

header.tmp - Temporary File. Delete.

interval.tmp - Temporary File. Delete.

windsp.tmp - Temporary File. Delete.

iseed.ran - Seed for the Random Number Generator Used to Determine Phase Angles.

(36)

APPENDIX E

DEFAULT PLOT SETUP

The first time the LIFE2 code is asked to plot data, a default hardware configuration is loaded. This configuration may be changed by the operator. The final configuration chosen by the operator is retained by code until it is manually changed by the operator.

At the first plot, the LIFE2 code displays the following message to alert the operator the default configuration has been loaded.

Warning: Plot parameters are not currently available,
default values are being loaded.

You may wish to review these parameters.

<Press Return to Continue>

The display default configuration is for a "CGA IBM Color Graphics Adapter." The x-axis is 6 inches long and start 1.5 inches from the bottom left-hand corner of the screen. The y-axis is 3 inches long and also starts 1.5 inches from the bottom left-hand corner of the screen. For 3-D plots, the azimuth and the elevation angles are relative to the preset values of 155° and 45°, respectively. The code lists this information in the follow form:

1) Hardware interface type:	99
2) Output device:	99
3) X-axis length:	6.0 in.
4) Y-axis length:	3.0 in.
5) X zero position:	1.5 in.
6) Y zero position:	1.5 in.
7) Azimuth rotation angle:	.0 deg.
8) Elevation rotation angle:	.0 deg.

The printer default configuration is for an "Epson 9 pin Printer," with an 8 inch carriage. The graph is plotted in double density. The printer is attached to "PRN" or "LPT1." The x-axis is 6 inches long and start 1.5 inches from the bottom left-hand corner of the page. The y-axis is 3 inches long and also starts 1.5 inches from the bottom left-hand corner of the screen. For 3D plots, the graphs are relative to the preset values of 155° and 45° for the azimuth and elevation angles, respectively. The code lists this information in the follow form:

1) Hardware interface type:	1
2) Output device:	1
3) X-axis length:	6.0 in.
4) Y-axis length:	3.0 in.
5) X zero position:	1.5 in.
6) Y zero position:	1.5 in.
7) Azimuth rotation angle:	.0 deg.
8) Elevation rotation angle:	.0 deg.

A typical setup for a "VGA" display configuration is given by

```
1) Hardware interface type:      97
2) Output device:                97
3) X-axis length:                6.0 in.
4) Y-axis length:                3.0 in.
5) X zero position:              1.5 in.
6) Y zero position:              1.5 in.
7) Azimuth rotation angle:        .0 deg.
8) Elevation rotation angle:      .0 deg.
```

A typical setup for a high density "HP Laserjet" plot is given by:

```
1) Hardware interface type:      1
2) Output device:                64
3) X-axis length:                6.0 in.
4) Y-axis length:                3.0 in.
5) X zero position:              1.5 in.
6) Y zero position:              1.5 in.
7) Azimuth rotation angle:        .0 deg.
8) Elevation rotation angle:      .0 deg.
```

A complete list of the hardware configurations supported by this plot package are listed in Appendix F.

APPENDIX F

HARDWARE CONFIGURATIONS FOR THE PLOTTING PACKAGE

The plot package used by the LIFE2 code is the PLOT88 Fortran plotting library. This package supports a large number of hardware configurations. These configurations are listed below.

PRINTER PORTS

ioport	Hardware interface types.
0	PRN: (PRN: is equivalent to LPT1:)
1	LPT1:
2	LPT2:
3	LPT3:

DISK FILE

ioport	Hardware interface types.
10	Disk File output. Deferred plotting mode.
11	Disk File output with carriage-return and line feed at the end of each line.

CONSOLE

ioport	Hardware interface types.
90,91,92	VGA IBM Video Graphics Array
93	HGC: Hercules Graphic Card
94,95,96,97	EGA IBM Enhanced Graphics Adapter
99	CGA IBM Color Graphics Adapter

SERIAL PORTS

ioport	device	baud rate	parity	#data bits	#stop bits
300	COM1:	300	N	8	1
301	COM1:	300	O	7	1
302	COM1:	300	E	7	1
1200	COM1:	1200	N	8	1
1201	COM1:	1200	O	7	1
1202	COM1:	1200	E	7	1
2400	COM1:	2400	N	8	1
2401	COM1:	2400	O	7	1
2402	COM1:	2400	E	7	1
4800	COM1:	4800	N	8	1
4801	COM1:	4800	O	7	1
4802	COM1:	4800	E	7	1
9600	COM1:	9600	N	8	1
9601	COM1:	9600	O	7	1
9602	COM1:	9600	E	7	1

parity: N = None E = Even O = Odd

COM2: = Add 50 to value for COM1:
For example, output to a device attached to COM2 with data transmitted at 9600 baud, 8 data bits, no parity would use an *ioport* value of 9600 + 50 = 9650.

PRINTERS

9 PIN DOT MATRIX PRINTERS

model	Output Device Identification
0	Epson 9 pin Printer, 8" carriage, single density.
1	Epson 9 pin Printer, 8" carriage, double density.
2	Epson 9 pin Printer, 8" carriage, double speed, dual density.
3	Epson 9 pin Printer, 8" carriage, quad density.
4	Epson 9 pin Printer, 8" carriage, CRT Graphics I.
5	Epson 9 pin Printer, 8" carriage, plotter graphics.
6	Epson 9 pin Printer, 8" carriage, CRT Graphics II.
10	Epson 9 pin Printer, 13.6" carriage, single density.
11	Epson 9 pin Printer, 13.6" carriage, double density.
12	Epson 9 pin Printer, 13.6" carriage, double speed, dual density.
13	Epson 9 pin Printer, 13.6" carriage, qauad density.
14	Epson 9 pin Printer, 13.6" carriage, CRT Graphics I.
15	Epson 9 pin Printer, 13.6" carriage, plotter graphics.
16	Epson 9 pin Printer, 13.6" carriage, CRT Graphics II.

FIXED ORIGIN HP PLOTTERS

20	HP 7470A Graphics Plotter (HPGL).
24	Fixed origin HPGL/2 printer & plotters.
30	HP 7475A Graphics Plotter or Enter Computer SP-600 Plotter. HP 7600 Model 240D and 240E Electrostatic plotters (HPGL).
	HP PaintJet XL Printer
35	180 dpi, A size page black & white
36	180 dpi, A size page, color
37	180 dpi, B size page, black & white
38	180 dpi, B size page, color

24 PIN DOT MATRIX PRINTERS

40	Epson 24 pin Printer. 13.6" carriage, single density.
41	Epson 24 pin Printer, 13.6" carriage, double density.
42	Epson 24 pin Printer, 13.6" carriage, double speed, dual density.
43	Epson 24 pin Printer, 13.6" carriage, quad density.
45	Epson 24 pin Printer, 8" carriage, single density.
46	Epson 24 pin Printer, 8" carriage, double density.
47	Epson 24 pin Printer, 8" carriage, double speed, dual density.
48	Epson 24 pin Printer, 8" carriage, quad density.

HOUSTON INSTRUMENT PLOTTERS

51	Houston Instrument DMP-51 MP, DMP-52 MP, DMP-56A, DMP-61, DM62, Enter SP1200, or Ioline LP 3700 Plotter, 0.001" step size. Paper sizes: A to D.
52	Houston Instrument DMP-51 MP, DMP-52 MP, DMP-56, DMP-61, DMP-62, or Enter SP1200 or Ioline LP 3700 Plotter, 0.005" step size.
56	Houston Instrument DMP-56, DMP-62, Enter SP1200 or Ioline LP 3700 Plotter, 0.001" step size. E size paper.

VARIABLE ORIGIN HP PLOTTERS

80	HP 7580B, HP 7585B, HP 7586B, HP 7575A, HP 7576A, HP 7595A, or HP 7596A Drafting Plotter, or Enter SP 1000 using size A/A4 to D/A1 paper. -HP DraftPro (7570A) Plotter using size C/A2 to D/A1 paper. -HP 7550A Graphics Plotter using size A/A4 to B/A3 paper. -HP ColorPro (7440A) plotter using size US/A4 paper.
81	Deferred output mode for HP plotters using A size paper.
82	Deferred output mode for HP plotters using B size paper.
83	Deferred output mode for HP plotters using C size paper.
84	Deferred output mode for HP plotters using D size paper.
85	-HP 7576A, HP 7585B, HP 7586B, HP 7595A, or HP 7596A Drafting Plotter using size E/A0 paper.
86	Deferred output mode for any HP plotter listed for model 85.

JET PRINTERS

Models 60 to 65 are used by the HP LaserJet, HP LaserJet Plus, HP LaserJet 500 Plus, the HP LaserJet Series II, HP LaserJet Series IID, IIP, HP DeskJet, DeskJet Plus.

60	HP LaserJet Printer using A size paper (8.5" x 11") (216 mm x 280 mm). Drawing resolution: 75 dots per inch.
61	HP LaserJet Printer, using B5 size paper (7.2" x 10.1") (182 mm x 257 mm). Drawing resolution: 75 dots per inch.
62	HP LaserJet Printer, using A size paper (8.5" x 11") (216 mm x 280 mm). Drawing resolution: 150 dots per inch.
63	HP LaserJet Printer, using B5 size paper (7.2" x 10.1") (182 mm x 257 mm). Drawing resolution: 150 dots per inch.
64	HP LaserJet Printer, using A size paper (8.5" x 11") (216 mm x 280 mm). Drawing resolution: 300 dots per inch.
65	HP LaserJet Printer, using B5 size paper (7.2" x 10.1") (182 mm x 257 mm). Drawing resolution: 300 dots per inch.
66	HP PaintJet (3630A) Printer, black and white, 90 dots per inch.
67	HP PaintJet (3630A) Printer, black and white, 180 dots per inch.
68	HP PaintJet (3630A) Printer, 16 colors from a palette of 330 90 dots per inch.
69	HP PaintJet (3630A) Printer, 16 colors fixed, 180 dots per inch.
70	HP ThinkJet (2225A) Printer, low density.
71	HP ThinkJet (2225A) Printer, high density.
72	HP QuietJet (2228A) Printer, single density.
73	HP QuietJet (2228A) Printer, double density.
74	HP QuietJet (2228A) Printer, quad density.

75	HP QuietJet Plus (2227A) Printer, single density.
76	HP QuietJet Plus (2227A) Printer, double density.
77	HP QuietJet Plus (2227A) Printer, quad density.

DISPLAYS

90, 91, 92	IBM Video Graphics Array (VGA)
93	Hercules graphics card (HGC).
94, 95, 96, 97	IBM Enhanced Graphics Adapter (EGA).
98, 99	IBM Color Graphics Adapter (CGA).

MISC

110	Color Encapsulated PostScript File 1000 dots per inch.
111	B/W Encapsulated PostScript File
112	Color Postscript Printer
113	B/W Postscript Printer
120	AutoCad DXF output file format.
122	CGM output, Binary mode
123	CGM output, Char encoding mode
124	CGM output, Clear Text mode

APPENDIX G

RECOMMENDED HARDWARE CONFIGURATIONS FOR THE PLOTTING PACKAGE

The recommended ioport and model for each device is as follows:

output device	ioport	model
Epson FX-80	0	5
Epson FX-80+	0	5
Epson JX-80	0	5
Epson FX-85	0	5
Epson FX-185	0	15
Epson FX-286	0	15
Epson MX-80	0	1
Epson RX-80	0	1
Epson FX-100	0	15
Epson FX-100+	0	15
Epson MX-100	0	11
Epson RX-100	0	11
Epson LQ-1500	0	41
IBM Graphics Printer	0	1
IBM ProPrinter	0	1
Centronics GLP	0	1
Okidata 92	0	1
Okidata 93	0	11
Okidata 182	0	1
Okidata 192	0	1
Okidata 193	0	11
HI DMP-51	9600/9650	51
HI DMP-52	9600/9650	51
HI DMP-56A	9600/9650	51
HI DMP-61	9600/9650	51
HI DMP-62	9600/9650	51
Enter SP-600	0	30
Enter SP-1000	9600/9650	80
Enter SP-1200	9600/9650	51
Ioline LP3700	9600/9650	51
HP 7440A	9600/9650	80
HP 7470A	9600/9650	20

HP 7475A	9600/9650	30
HP 7550A	9600/9650	80
HP 7570A	9600/9650	80
HP 7575A	9600/9650	80
HP 7576A	9600/9650	80
HP 7580B	9600/9650	80
HP 7585B	9600/9650	80/85
HP 7586B	9600/9650	80/85
HP 7595A	9600/9650	80/85
HP 7596A	9600/9650	80/85
HP 7600/240D	0	30
HP 7600/240E	0	30
HP 3630A	0	68
HP ThinkJet (2225A)	0	70
HP QuietJet (2228A)	0	72
HP QuietJet Plus (2227A)	0	75
HP DeskJet (2276A)	0	60/61
HP LaserJet Printers	9600/9650/0	60/61
HP PaintJet XL	9600/9650/0	36/38
Hercules Graphics Card	93	93
IBM EGA	96 or 97	96 or 97
IBM Color Graphics Adapter	99	99
IBM VGA	91	91
PostScript Encapsulated	11	110
PostScript Printer	9600/9650/0	112
AutoCad	11	120
CGM, Character Encoding	10	123
CGM, Clear Text	11	124
CGM, Binary mode	10	122

DISTRIBUTION:

R. E. Akins
Washington & Lee University
P.O. Box 735
Lexington, VA 24450

M. Anderson
Renewable Energy Systems, Ltd.
Eaton Court, Maylands Avenue
Hemel Hempstead
Herts HP2 7DR
ENGLAND

H. Ashley
Dept. of Aeronautics and
Astronautics Mechanical Engr.
Stanford University
Stanford, CA 94305

C. P. Butterfield
NREL
1617 Cole Blvd.
Golden, CO 80401

G. Bywaters
Northern Power Systems
Box 659
Moretown, VT 05660

R. N. Clark
USDA
Agricultural Research Service
Southwest Great Plains Research
Center
Bushland, TX 79012

C. Coleman
Northern Power Systems
Box 659
Moretown, VT 05660

O. Dyes
Wind/Hydro/Ocean Div.
U.S. Department of Energy
1000 Independence Avenue, SW
Washington, DC 20585

A. J. Eggers, Jr.
RANN, Inc.
260 Sheridan Ave., Suite 414
Palo Alto, CA 94306

D. Eggleston
DME Engineering
P.O. Box 5907
Midland, TX 79704-5907

P. R. Goldman
Wind/Hydro/Ocean Division
U.S. Department of Energy
1000 Independence Avenue
Washington, DC 20585

I. J. Graham
Dept. of Mechanical Engineering
Southern University
P.O. Box 9445
Baton Rouge, LA 70813-9445

G. Gregorek
Aeronautical & Astronautical
Dept.
Ohio State University
2300 West Case Road
Columbus, OH 43220

C. Hansen
University of Utah
Department of Mechanical Engr.
Salt Lake City, UT 84112

R. Heffernan
U.S. WindPower
6952 Preston Avenue
Livermore, CA 94550

L. Helling
Librarian
National Atomic Museum
Albuquerque, NM 87185

T. Hillesland
Pacific Gas and Electric Co.
3400 Crow Canyon Road
San Ramon, CA 94583

S. Hock
Wind Energy Program
NREL
Boulder, CO 80401

W. E. Holley
U.S. WindPower
6952 Preston Avenue
Livermore, CA 94550

M. A. Ilyan
Pacific Gas and Electric Co.
3400 Crow Canyon Road
San Ramon, CA 94583

B. J. Im
McGillim Research
4903 Wagonwheel Way
El Sobrante, CA 94803

K. Jackson
Dynamic Design
123 C Street
Davis, CA 95616

L. Jea
Loral Vought Systems
Mail Stop SP79
P.O. Box 650003
Dallas, TX 75265-0003

O. Krauss
Division of Engineering Research
Michigan State University
East Lansing, MI 48825

C. Lange
Civil Engineering Dept.
Stanford University
Stanford, CA 94305

G. G. Leigh
New Mexico Engineering
Research Institute
Campus P.O. Box 25
Albuquerque, NM 87131

A. Liniecki
Mech. Engineering Dept.
One Washington Square
San Jose, CA 95192

R. Lynette
R. Lynette & Assoc., Inc.
15042 NE 40th Street
Suite 206
Redmond, WA 98052

P. H. Madsen
Riso National Laboratory
Postbox 49
DK-4000 Roskilde
DENMARK

D. Malcolm
R. Lynette & Associates, Inc.
15042 N.E. 40th Street, Suite
206
Redmond, WA 98052

J. F. Mandell
Montana State University
302 Cableigh Hall
Bozeman, MT 59717

G. McNerney
U.S. Windpower, Inc.
6952 Preston Avenue
Livermore, CA 94550

A. Mikhail
Zond Systems, Inc.
13000 Jameson Rd.
P.O. Box 1910
Tehachapi, CA 93561

S. Miller
162636 NE 19th Place
Bellevue, WA 98008-2552

R. H. Monroe
Gougeon Brothers
100 Patterson Avenue
Bay City, MI 48706

D. Morrison
New Mexico Engineering
Research Institute
Campus P.O. Box 25
Albuquerque, NM 87131

V. Nelson
Department of Physics
West Texas State University
P.O. Box 248
Canyon, TX 79016

G. Nix
NREL
1617 Cole Boulevard
Golden, CO 80401

J. W. Oler
Mechanical Engineering Dept.
Texas Tech University
P.O. Box 4289
Lubbock, TX 79409

R. Osgood
NREL
1617 Cole Blvd.
Golden, CO 80401

C. Paquette
The American Wind Energy
Association
777 N. Capitol Street, NE
Suite 805
Washington, DC 20002

R. G. Rajagopalan
Aerospace Engineering
Department
Iowa State University
404 Town Engineering Bldg.
Ames, IA 50011

R. Rangi
Manager, Wind Technology
Dept. of Energy, Mines and
Resources
580 Booth 7th Floor
Ottawa, Ontario K1A 0E4
CANADA

M. G. Real, President
Alpha Real Ag
Feldeggstrasse 89
CH 8008 Zurich
SWITZERLAND

R. L. Scheffler
Research and Development Dept.
Room 497
Southern California Edison
P.O. Box 800
Rosemead, CA 91770

L. Schienbein
Battelle-Pacific Northwest
Laboratory
P.O. Box 999
Richland, WA 99352

T. Schweizer
Princeton Economic Research,
Inc.
12300 Twinbrook Parkway
Suite 650
Rockville, MD 20852

J. Sladky, Jr.
Kinetics Group, Inc.
P.O. Box 1071
Mercer Island, WA 98040

M. Snyder
Aero Engineering Department
Wichita State University
Wichita, KS 67208

K. Starcher
AEI
West Texas State University
P.O. Box 248
Canyon, TX 79016

F. S. Stoddard
Second Wind, Inc.
7 Davis Square
Somerville, MA 02144

D. Taylor
Alternative Energy Group
Walton Hall
Open University
Milton Keynes MK7 6AA
UNITED KINGDOM

G. P. Tennyson
DOE/AL/ETWMD
Albuquerque, NM 87115

W. V. Thompson
410 Ericwood Court
Manteca, CA 95336

R. W. Thresher
NREL
1617 Cole Boulevard
Golden, CO 80401

W. A. Vachon
W. A. Vachon & Associates
P.O. Box 149
Manchester, MA 01944

B. Vick
68110 Club Circle Dr.
Desert Hot Springs, CA 92240

V. Wallace
FloWind Corp.
990 A Street, Suite 300
San Rafael, CA 94901

L. Wendell
Battelle-Pacific Northwest
Laboratory
P.O. Box 999
Richland, WA 99352

R. E. Wilson
Mechanical Engineering Dept.
Oregon State University
Corvallis, OR 97331

S. Winterstein
Civil Engineering Dept.
Stanford University
Stanford, CA 94305

R. Yetka
EM&A Dept.
2348 Engineering Hall
1415 Johnson Dr.
Madison, WI 53706-1691

M. Zuteck
MDZ Consulting
931 Grove Street
Kemah, TX 77565

1434 C. Dohrmann
1434 D. W. Lobitz
1434 D. R. Martinez
1561 J. G. Arguello
1562 E. D. Reedy
2741 T. G. Carne
2741 G. H. James III
6214 H. M. Dodd (50)
6214 T. D. Ashwill
6214 D. E. Berg
6214 M. A. Rumsey
6214 L. L. Schluter
6214 H. J. Sutherland
6214 P. S. Veers
7141 Technical Library (5)
7151 Technical Publications
7161 J. C. Clausen
7613-2 Document Processing(10)
For DOE/OSTI
8523-2 Central Technical Files

NMERI R. L. Linker (10)
NMERI D. Burwinkle

DATE FILMED

1/31/94

END